


Search for Unstable Sterile Neutrinos with the IceCube Neutrino Observatory

R. Abbasi,¹⁷ M. Ackermann,⁶¹ J. Adams,¹⁸ J. A. Aguilar,¹² M. Ahlers,²² M. Ahrens,⁵¹ J. M. Alameddine,²³ A. A. Alves, Jr.,³¹ N. M. Amin,⁴³ K. Andeen,⁴¹ T. Anderson,⁵⁸ G. Anton,²⁶ C. Argüelles,¹⁴ Y. Ashida,³⁹ S. Axani,¹⁵ X. Bai,⁴⁷ A. Balagopal V.,³⁹ S. W. Barwick,³⁰ B. Bastian,⁶¹ V. Basu,³⁹ S. Baur,¹² R. Bay,⁸ J. J. Beatty,^{20,21} K.-H. Becker,⁶⁰ J. Becker Tjus,¹¹ J. Beise,⁵⁹ C. Bellenghi,²⁷ S. Benda,³⁹ S. BenZvi,⁴⁹ D. Berley,¹⁹ E. Bernardini,^{61,†} D. Z. Besson,³⁴ G. Binder,^{8,9} D. Bindig,⁶⁰ E. Blaufuss,¹⁹ S. Blot,⁶¹ M. Boddenberg,¹ F. Bontempo,³¹ J. Y. Book,¹⁴ J. Borowka,¹ S. Böser,⁴⁰ O. Botner,⁵⁹ J. Böttcher,¹ E. Bourbeau,²² F. Bradascio,⁶¹ J. Braun,³⁹ B. Brinson,⁶ S. Bron,²⁸ J. Brostean-Kaiser,⁶¹ R. T. Burley,² R. S. Busse,⁴² M. A. Campana,⁴⁶ E. G. Carnie-Bronca,² C. Chen,⁶ Z. Chen,⁵² D. Chirkin,³⁹ K. Choi,⁵³ B. A. Clark,²⁴ K. Clark,³³ L. Classen,⁴² A. Coleman,⁴³ G. H. Collin,¹⁵ J. M. Conrad,¹⁵ P. Coppin,¹³ P. Correa,¹³ D. F. Cowen,^{57,58} R. Cross,⁴⁹ C. Dappen,¹ P. Dave,⁶ C. De Clercq,¹³ J. J. DeLaunay,⁵⁶ D. Delgado López,¹⁴ H. Dembinski,⁴³ K. Deoskar,⁵¹ A. Desai,³⁹ P. Desiati,³⁹ K. D. de Vries,¹³ G. de Wasseige,³⁶ M. de With,¹⁰ T. DeYoung,²⁴ A. Diaz,¹⁵ J. C. Díaz-Vélez,³⁹ M. Dittmer,⁴² H. Dujmovic,³¹ M. Dunkman,⁵⁸ M. A. DuVernois,³⁹ T. Ehrhardt,⁴⁰ P. Eller,²⁷ R. Engel,^{31,32} H. Erpenbeck,¹ J. Evans,¹⁹ P. A. Evenson,⁴³ K. L. Fan,¹⁹ A. R. Fazely,⁷ A. Fedynitch,⁵⁵ N. Feigl,¹⁰ S. Fiedlschuster,²⁶ A. T. Fienberg,⁵⁸ C. Finley,⁵¹ L. Fischer,⁶¹ D. Fox,⁵⁷ A. Franckowiak,^{11,61} E. Friedman,¹⁹ A. Fritz,⁴⁰ P. Fürst,¹ T. K. Gaisser,⁴³ J. Gallagher,³⁸ E. Ganster,¹ A. Garcia,¹⁴ S. Garrappa,⁶¹ L. Gerhardt,⁹ A. Ghadimi,⁵⁶ C. Glaser,⁵⁹ T. Glauch,²⁷ T. Glüsenkamp,²⁶ N. Goehlike,³² J. G. Gonzalez,⁴³ S. Goswami,⁵⁶ D. Grant,²⁴ T. Grégoire,⁵⁸ S. Griswold,⁴⁹ C. Günther,¹ P. Gutjahr,²³ C. Haack,²⁷ A. Hallgren,⁵⁹ R. Halliday,²⁴ L. Halve,¹ F. Halzen,³⁹ M. Ha Minh,²⁷ K. Hanson,³⁹ J. Hardin,³⁹ A. A. Harnisch,²⁴ A. Haungs,³¹ D. Hebecker,¹⁰ K. Helbing,⁶⁰ F. Henningsen,²⁷ E. C. Hettinger,²⁴ S. Hickford,⁶⁰ J. Hignight,²⁵ C. Hill,¹⁶ G. C. Hill,² K. D. Hoffman,¹⁹ K. Hoshina,^{39,‡} W. Hou,³¹ F. Huang,⁵⁸ M. Huber,²⁷ T. Huber,³¹ K. Hultqvist,⁵¹ M. Hünnefeld,²³ R. Hussain,³⁹ K. Hymon,²³ S. In,⁵³ N. Iovine,¹² A. Ishihara,¹⁶ M. Jansson,⁵¹ G. S. Japaridze,⁵ M. Jeong,⁵³ M. Jin,¹⁴ B. J. P. Jones,⁴ D. Kang,³¹ W. Kang,⁵³ X. Kang,⁴⁶ A. Kappes,⁴² D. Kappesser,⁴⁰ L. Kardum,²³ T. Karg,⁶¹ M. Karl,²⁷ A. Karle,³⁹ U. Katz,²⁶ M. Kauer,³⁹ M. Kellermann,¹ J. L. Kelley,³⁹ A. Kheirandish,⁵⁸ K. Kin,¹⁶ T. Kintscher,⁶¹ J. Kiryluk,⁵² S. R. Klein,^{8,9} A. Kochocki,²⁴ R. Koirala,⁴³ H. Kolanoski,¹⁰ T. Kontrimas,²⁷ L. Köpke,⁴⁰ C. Kopper,²⁴ S. Kopper,⁵⁶ D. J. Koskinen,²² P. Koundal,³¹ M. Kovacevich,⁴⁶ M. Kowalski,^{10,61} T. Kozynets,²² E. Krupczak,²⁴ E. Kun,¹¹ N. Kurahashi,⁴⁶ N. Lad,⁶¹ C. Lagunas Gualda,⁶¹ J. L. Lanfranchi,⁵⁸ M. J. Larson,¹⁹ F. Lauber,⁶⁰ J. P. Lazar,^{14,39} J. W. Lee,⁵³ K. Leonard,³⁹ A. Leszczyńska,⁴³ Y. Li,⁵⁸ M. Lincetto,¹¹ Q. R. Liu,³⁹ M. Liubarska,²⁵ E. Lohfink,⁴⁰ C. J. Lozano Mariscal,⁴² L. Lu,³⁹ F. Lucarelli,²⁸ A. Ludwig,^{24,35} W. Luszczak,³⁹ Y. Lyu,^{8,9} W. Y. Ma,⁶¹ J. Madsen,³⁹ K. B. M. Mahn,²⁴ Y. Makino,³⁹ S. Mancina,³⁹ I. C. Mariş,¹² I. Martinez-Soler,¹⁴ R. Maruyama,⁴⁴ S. McCarthy,³⁹ T. McElroy,²⁵ F. McNally,³⁷ J. V. Mead,²² K. Meagher,³⁹ S. Mechbal,⁶¹ A. Medina,²¹ M. Meier,¹⁶ S. Meighen-Berger,²⁷ J. Micallef,²⁴ D. Mockler,¹² T. Montaruli,²⁸ R. W. Moore,²⁵ R. Morse,³⁹ M. Moulai,¹⁵ T. Mukherjee,³¹ R. Naab,⁶¹ R. Nagai,¹⁶ U. Naumann,⁶⁰ J. Necker,⁶¹ L. V. Nguyễn,²⁴ H. Niederhausen,²⁴ M. U. Nisa,²⁴ S. C. Nowicki,²⁴ A. Obertacke Pollmann,⁶⁰ M. Oehler,³¹ B. Oeyen,²⁹ A. Olivas,¹⁹ E. O'Sullivan,⁵⁹ H. Pandya,⁴³ D. V. Pankova,⁵⁸ N. Park,³³ G. K. Parker,⁴ E. N. Paudel,⁴³ L. Paul,⁴¹ C. Pérez de los Heros,⁵⁹ L. Peters,¹ J. Peterson,³⁹ S. Philippen,¹ S. Pieper,⁶⁰ A. Pizzuto,³⁹ M. Plum,⁴⁷ Y. Popovych,⁴⁰ A. Porcelli,²⁹ M. Prado Rodriguez,³⁹ B. Pries,²⁴ G. T. Przybylski,⁹ C. Raab,¹² J. Rack-Helleis,⁴⁰ A. Raissi,¹⁸ M. Rameez,²² K. Rawlins,³ I. C. Rea,²⁷ Z. Rechav,³⁹ A. Rehman,⁴³ P. Reichherzer,¹¹ R. Reimann,¹ G. Renzi,¹² E. Resconi,²⁷ S. Reusch,⁶¹ W. Rhode,²³ M. Richman,⁴⁶ B. Riedel,³⁹ E. J. Roberts,² S. Robertson,^{8,9} G. Roellinghoff,⁵³ M. Rongen,⁴⁰ C. Rott,^{50,53} T. Ruhe,²³ D. Ryckbosch,²⁹ D. Rysewyk Cantu,²⁴ I. Safa,^{14,39} J. Saffer,³² P. Sampathkumar,³¹ S. E. Sanchez Herrera,²⁴ A. Sandrock,²³ M. Santander,⁵⁶ S. Sarkar,⁴⁵ S. Sarkar,²⁵ K. Satalecka,⁶¹ M. Schaufel,¹ H. Schieler,³¹ S. Schindler,²⁶ T. Schmidt,¹⁹ A. Schneider,³⁹ J. Schneider,²⁶ F. G. Schröder,^{31,43} L. Schumacher,²⁷ G. Schwefer,¹ S. Sclafani,⁴⁶ D. Seckel,⁴³ S. Seunarine,⁴⁸ A. Sharma,⁵⁹ S. Shefali,³² N. Shimizu,¹⁶ M. Silva,³⁹ B. Skrzypek,¹⁴ B. Smithers,⁴ R. Snihur,³⁹ J. Soedingrekso,²³ D. Soldin,⁴³ C. Spannfellner,²⁷ G. M. Spiczak,⁴⁸ C. Spiering,⁶¹ J. Stachurska,⁶¹ M. Stamatikos,²¹ T. Stanev,⁴³ R. Stein,⁶¹ J. Stettner,¹ T. Stezelberger,⁹ T. Stürwald,⁶⁰ T. Stuttard,²² G. W. Sullivan,¹⁹ I. Taboada,⁶ S. Ter-Antonyan,⁷ J. Thwaites,³⁹ S. Tilav,⁴³ F. Tischbein,¹ K. Tollefson,²⁴ C. Tönnis,⁵⁴ S. Toscano,¹² D. Tosi,³⁹ A. Trettin,⁶¹ M. Tselengidou,²⁶ C. F. Tung,⁶ A. Turcati,²⁷ R. Turcotte,³¹ C. F. Turley,⁵⁸ J. P. Twagirayezu,²⁴ B. Ty,³⁹ M. A. Unland Elorrieta,⁴² N. Valtonen-Mattila,⁵⁹ J. Vandenbroucke,³⁹ N. van Eijndhoven,¹³ D. Vannerom,¹⁵ J. van Santen,⁶¹ J. Veitch-Michaelis,³⁹ S. Verpoest,²⁹ C. Walck,²³ W. Wang,³⁹ T. B. Watson,⁴ C. Weaver,²⁴ P. Weigel,¹⁵ A. Weindl,³¹ M. J. Weiss,⁵⁸ J. Weldert,⁴⁰ C. Wendt,³⁹ J. Werthebach,²³ M. Weyrauch,³¹ N. Whitehorn,^{24,35} C. H. Wiebusch,¹ N. Willey,²⁴ D. R. Williams,⁵⁶ M. Wolf,³⁹ G. Wrede,²⁶ J. Wulff,¹¹ X. W. Xu,⁷ J. P. Yanez,²⁵ E. Yildizci,³⁹ S. Yoshida,¹⁶ S. Yu,²⁴ T. Yuan,³⁹ Z. Zhang,⁵² and P. Zhelнин¹⁴

(IceCube Collaboration)*

- ¹III. Physikalisches Institut, RWTH Aachen University, D-52056 Aachen, Germany
- ²Department of Physics, University of Adelaide, Adelaide 5005, Australia
- ³Department of Physics and Astronomy, University of Alaska Anchorage, 3211 Providence Dr., Anchorage, Alaska 99508, USA
- ⁴Department of Physics, University of Texas at Arlington, 502 Yates Street, Science Hall Rm 108, Box 19059, Arlington, Texas 76019, USA
- ⁵CTSPS, Clark-Atlanta University, Atlanta, Georgia 30314, USA
- ⁶School of Physics and Center for Relativistic Astrophysics, Georgia Institute of Technology, Atlanta, Georgia 30332, USA
- ⁷Department of Physics, Southern University, Baton Rouge, Louisiana 70813, USA
- ⁸Department of Physics, University of California, Berkeley, California 94720, USA
- ⁹Lawrence Berkeley National Laboratory, Berkeley, California 94720, USA
- ¹⁰Institut für Physik, Humboldt-Universität zu Berlin, D-12489 Berlin, Germany
- ¹¹Fakultät für Physik & Astronomie, Ruhr-Universität Bochum, D-44780 Bochum, Germany
- ¹²Université Libre de Bruxelles, Science Faculty CP230, B-1050 Brussels, Belgium
- ¹³Vrije Universiteit Brussel (VUB), Dienst ELEM, B-1050 Brussels, Belgium
- ¹⁴Department of Physics and Laboratory for Particle Physics and Cosmology, Harvard University, Cambridge, Massachusetts 02138, USA
- ¹⁵Department of Physics, Massachusetts Institute of Technology, Cambridge, Massachusetts 02139, USA
- ¹⁶Department of Physics and The International Center for Hadron Astrophysics, Chiba University, Chiba 263-8522, Japan
- ¹⁷Department of Physics, Loyola University Chicago, Chicago, Illinois 60660, USA
- ¹⁸Department of Physics and Astronomy, University of Canterbury, Private Bag 4800, Christchurch, New Zealand
- ¹⁹Department of Physics, University of Maryland, College Park, Maryland 20742, USA
- ²⁰Department of Astronomy, Ohio State University, Columbus, Ohio 43210, USA
- ²¹Department of Physics and Center for Cosmology and Astro-Particle Physics, Ohio State University, Columbus, Ohio 43210, USA
- ²²Niels Bohr Institute, University of Copenhagen, DK-2100 Copenhagen, Denmark
- ²³Department of Physics, TU Dortmund University, D-44221 Dortmund, Germany
- ²⁴Department of Physics and Astronomy, Michigan State University, East Lansing, Michigan 48824, USA
- ²⁵Department of Physics, University of Alberta, Edmonton, Alberta, Canada T6G 2E1
- ²⁶Erlangen Centre for Astroparticle Physics, Friedrich-Alexander-Universität Erlangen-Nürnberg, D-91058 Erlangen, Germany
- ²⁷Physik-department, Technische Universität München, D-85748 Garching, Germany
- ²⁸Département de physique nucléaire et corpusculaire, Université de Genève, CH-1211 Genève, Switzerland
- ²⁹Department of Physics and Astronomy, University of Gent, B-9000 Gent, Belgium
- ³⁰Department of Physics and Astronomy, University of California, Irvine, California 92697, USA
- ³¹Karlsruhe Institute of Technology, Institute for Astroparticle Physics, D-76021 Karlsruhe, Germany
- ³²Karlsruhe Institute of Technology, Institute of Experimental Particle Physics, D-76021 Karlsruhe, Germany
- ³³Department of Physics, Engineering Physics, and Astronomy, Queen's University, Kingston, Ontario K7L 3N6, Canada
- ³⁴Department of Physics and Astronomy, University of Kansas, Lawrence, Kansas 66045, USA
- ³⁵Department of Physics and Astronomy, UCLA, Los Angeles, California 90095, USA
- ³⁶Centre for Cosmology, Particle Physics and Phenomenology - CP3, Université catholique de Louvain, B-1348 Louvain-la-Neuve, Belgium
- ³⁷Department of Physics, Mercer University, Macon, Georgia 31207-0001, USA
- ³⁸Department of Astronomy, University of Wisconsin–Madison, Madison, Wisconsin 53706, USA
- ³⁹Department of Physics and Wisconsin IceCube Particle Astrophysics Center, University of Wisconsin–Madison, Madison, Wisconsin 53706, USA
- ⁴⁰Institute of Physics, University of Mainz, Staudinger Weg 7, D-55099 Mainz, Germany
- ⁴¹Department of Physics, Marquette University, Milwaukee, Wisconsin 53201, USA
- ⁴²Institut für Kernphysik, Westfälische Wilhelms-Universität Münster, D-48149 Münster, Germany
- ⁴³Bartol Research Institute and Department of Physics and Astronomy, University of Delaware, Newark, Delaware 19716, USA
- ⁴⁴Department of Physics, Yale University, New Haven, Connecticut 06520, USA
- ⁴⁵Department of Physics, University of Oxford, Parks Road, Oxford OX1 3PU, United Kingdom
- ⁴⁶Department of Physics, Drexel University, 3141 Chestnut Street, Philadelphia, Pennsylvania 19104, USA
- ⁴⁷Physics Department, South Dakota School of Mines and Technology, Rapid City, South Dakota 57701, USA
- ⁴⁸Department of Physics, University of Wisconsin, River Falls, Wisconsin 54022, USA
- ⁴⁹Department of Physics and Astronomy, University of Rochester, Rochester, New York 14627, USA
- ⁵⁰Department of Physics and Astronomy, University of Utah, Salt Lake City, Utah 84112, USA
- ⁵¹Oskar Klein Centre and Department of Physics, Stockholm University, SE-10691 Stockholm, Sweden
- ⁵²Department of Physics and Astronomy, Stony Brook University, Stony Brook, New York 11794-3800, USA
- ⁵³Department of Physics, Sungkyunkwan University, Suwon 16419, Korea

⁵⁴*Institute of Basic Science, Sungkyunkwan University, Suwon 16419, Korea*⁵⁵*Institute of Physics, Academia Sinica, Taipei 11529, Taiwan*⁵⁶*Department of Physics and Astronomy, University of Alabama, Tuscaloosa, Alabama 35487, USA*⁵⁷*Department of Astronomy and Astrophysics, Pennsylvania State University, University Park, Pennsylvania 16802, USA*⁵⁸*Department of Physics, Pennsylvania State University, University Park, Pennsylvania 16802, USA*⁵⁹*Department of Physics and Astronomy, Uppsala University, Box 516, S-75120 Uppsala, Sweden*⁶⁰*Department of Physics, University of Wuppertal, D-42119 Wuppertal, Germany*⁶¹*DESY, D-15738 Zeuthen, Germany* (Received 6 April 2022; revised 17 August 2022; accepted 23 August 2022; published 7 October 2022)

We present a search for an unstable sterile neutrino by looking for a resonant signal in eight years of atmospheric ν_μ data collected from 2011 to 2019 at the IceCube Neutrino Observatory. Both the (stable) three-neutrino and the $3 + 1$ sterile neutrino models are disfavored relative to the unstable sterile neutrino model, though with p values of 2.8% and 0.81%, respectively, we do not observe evidence for $3 + 1$ neutrinos with neutrino decay. The best-fit parameters for the sterile neutrino with decay model from this study are $\Delta m_{41}^2 = 6.7_{-2.5}^{+3.9}$ eV², $\sin^2 2\theta_{24} = 0.33_{-0.17}^{+0.20}$, and $g^2 = 2.5\pi \pm 1.5\pi$, where g is the decay-mediating coupling. The preferred regions of the $3 + 1 +$ decay model from short-baseline oscillation searches are excluded at 90% C.L.

DOI: [10.1103/PhysRevLett.129.151801](https://doi.org/10.1103/PhysRevLett.129.151801)

Long-standing anomalies in short-baseline (SBL) neutrino experiments [1,2] have been interpreted in the standard oscillation framework of three known flavors and one or more hypothetical sterile neutrinos, referred to as “ $3 + N$ ” models. The “ $3 + 1$ ” model, which involves only one sterile neutrino, has been extensively studied through global fits to datasets sensitive to vacuum oscillations involving a dominant mass splitting of ~ 1 eV² [3–5]. These fits find a strong preference for $3 + 1$ over the three neutrino hypothesis [4]. However, the allowed regions from these fits suffer from internal inconsistencies between datasets [4,6]. In particular, no experiment has found evidence of ν_μ disappearance, which is expected in a $3 + 1$ model. This is one motivation to consider alternative models to the $3 + 1$; another is to evade cosmological bounds on light sterile neutrinos [7–11] and possibly resolve the Hubble tension [12–16].

Other explanations for the observed anomalies include misestimation of standard model backgrounds in the experiments with anomalies [2,17–20], alternative models that do not involve light sterile neutrinos [21–32], and extensions to the $3 + 1$ model that address the internal tension [33–35]. In the latter case, models wherein the sterile neutrino is unstable (“ $3 + 1 +$ decay”) reduce the tension compared to the $3 + 1$ model [4,35,36]. However, to be seen as a well-motivated improvement, the $3 + 1 +$ decay model should be tested through entirely different processes than vacuum oscillations.

The IceCube Neutrino Observatory has the unique capability of performing such a test. IceCube is a cubic-kilometer neutrino detector buried 1.5–2.5 km beneath the surface of the Antarctic glacier at the South Pole [37]. Muon tracks from charged current (CC) muon (anti)neutrino interactions are reconstructed based on observation of emitted Cherenkov light that is collected by “digital optical modules” (DOMs) [38] arranged in vertical strings on a hexagonal lattice. Specifically, the track fitting [39] utilizes signals from two detector arrays: (i) the main array of 78 strings spaced 125 m apart, each carrying 60 DOMs with a vertical separation of 17 m between them; and (ii) the DeepCore [40] eight-string array, with lateral spacing varying from 42 to 72 m, and vertical DOM separation of 7 m.

The existence of an eV-scale sterile neutrino can manifest itself as a resonant, matter-enhanced flavor transition for either muon antineutrinos or muon neutrinos traversing the core of the Earth [41–46]. This causes a deficit of “up-going” muon (anti)neutrinos at TeV-scale energies. IceCube cannot distinguish between neutrinos and antineutrinos. Therefore, the only signature is a deficit in the combined muon neutrino and muon antineutrino ($\nu_\mu + \bar{\nu}_\mu$) CC event distribution at TeV energies. A search in the framework of the $3 + 1$ model using eight years of IceCube data has recently been published [47,48]. This dataset offers an excellent platform to test the hypothesis that the $3 + 1 +$ decay model provides a better description of the data than the $3 + 1$ model without relying upon the vacuum oscillation signature.

In the $3 + 1 +$ decay model, the three-neutrino mixing matrix, U_{PNMS} , which is parametrized by three mixing angles and one CP -violating phase, δ_{CP} , is extended by one row and column, adding one sterile flavor state, ν_s , and one heavy mass state, ν_4 . This introduces three new mixing angles, θ_{14} , θ_{24} , and θ_{34} , two new CP -violating phases, δ_{14}

Published by the American Physical Society under the terms of the [Creative Commons Attribution 4.0 International license](https://creativecommons.org/licenses/by/4.0/). Further distribution of this work must maintain attribution to the author(s) and the published article’s title, journal citation, and DOI. Funded by SCOAP³.

and δ_{24} , and one additional mass splitting, Δm_{41}^2 . Lastly, instability of the fourth mass state is introduced as in Ref. [4], governed by the strength of a coupling constant g . For nonzero values of g , ν_4 can decay into invisible particles beyond the standard model, while $g = 0$ returns the $3 + 1$ model. The relationship between this coupling, g , the ν_4 mass, m_4 , and its lifetime, τ , is [49]

$$\tau = \frac{16\pi}{g^2 m_4}. \quad (1)$$

Most of the parameters involved in three-neutrino mixing are well known; these include the light, active neutrino mass splittings and the PMNS matrix elements [50]. However, this Letter is insensitive to these parameters as well as to the neutrino mass ordering and δ_{CP} because, for the relevant neutrino energies ($E_\nu > 100$ GeV) and baselines (order the diameter of the Earth or smaller), oscillation probabilities between the three active flavors are insignificant. For the present study, the normal mass ordering is assumed and δ_{CP} is assumed to be zero. Furthermore θ_{14} , δ_{14} , and δ_{24} are set to zero since they have subleading effects [51]; θ_{34} is set to zero as this yields conservative results [51,52] and m_1 is set to zero since only mass differences are relevant. This leaves three free parameters in the model to be tested: Δm_{41}^2 , $\sin^2 2\theta_{24}$, and g^2 . It is assumed that $\theta_{24} < \pi/4$, which causes the resonance to appear in the antineutrino flux; larger values of θ_{24} are heavily constrained [4] and since there are more atmospheric neutrinos than antineutrinos [53], this choice is also conservative.

At IceCube, the ν_μ and $\bar{\nu}_\mu$ disappearance probabilities vary as a function of energy and zenith angle (θ_z), where $\cos \theta_z = 0$ corresponds to neutrinos arriving from the horizon and $\cos \theta_z = -1$ corresponds to neutrinos arriving from the direction of the North Pole. This study uses a dataset collected over a live time of 2786 days and an event selection that has been described in detail in Refs. [48,54]. The predicted resonance occurs at TeV scales, hence the analysis focuses on muons from CC neutrino interactions with energies between 500 GeV and 10 TeV. Relevant neutrino interactions occur below or within IceCube. Because the signature of the analysis relies on matter effects in the Earth, this analysis requires muon tracks to have up-going zenith angle ($-1.0 < \cos \theta_z < 0.0$). The angular resolution of the tracks, $\sigma_{\cos \theta_z}$, lies between 0.005 and 0.015, and the track energy resolution, $\sigma_{\log_{10}(E_\mu/\text{GeV})}$, is ~ 0.5 [39]. The selected sample comprises 305 735 CC ν_μ and $\bar{\nu}_\mu$ events.

The expected neutrino flux is primarily atmospheric neutrinos, with approximately a 3% overall contribution from astrophysical neutrinos, determined by extrapolating from measurements at higher energies [55–61]. The atmospheric flux arises predominantly from the decays of kaons and pions, and to a much lesser extent, muons, in cosmic-ray air showers [62]. The decays of heavier mesons contribute minimally to the atmospheric flux in the energy

range relevant to this analysis [63–69]. The atmospheric and astrophysical fluxes fall steeply with energy, with spectral indices of approximately -3.7 and -2.5 , respectively [61,70].

The physics under study affects the flavors of the neutrinos as they propagate through the Earth. This is described using the nuSQUIDS neutrino evolution code [71,72] which accounts for both coherent and incoherent interactions [73–78], as well as tau neutrino regeneration [79,80]. This analysis uses nuSQUIDSDecay, which incorporates the effect of ν_4 decay [34]. The Earth density profile is parametrized by the spherically symmetric PREM model [81]. The CSMS [82] neutrino-nucleon cross section is used to describe the CC interactions below and within the detector.

This analysis builds on the $3 + 1$ analysis in Ref. [48]. The data are binned in reconstructed muon energy and $\cos \theta_z$, and a modified Poisson likelihood that accounts for finite simulation statistics is used to evaluate the data given sterile neutrino parameters [83]. Eighteen systematic effects related to the atmospheric and astrophysical flux, detector, and cross section uncertainties are incorporated into the likelihood function as nuisance parameters; these are described further in Ref. [48]. The treatment of most systematic uncertainties is unchanged. The dominant category of uncertainties had been identified as those associated with the atmospheric neutrino flux.

Two improvements were made over the $3 + 1$ analysis: (i) the uncertainty in the atmospheric neutrino flux corresponding to the uncertainty in the production of charged mesons in atmospheric showers is calculated using atmospheric data from the NASA Atmospheric InfraRed Sounder satellite [84], rather than the atmospheric model from Ref. [85]; and (ii) the astrophysical and prompt neutrino fluxes are calculated using a corrected depth setting of the glacial ice, compared to Ref. [48], which had little impact on the current or previous results. Combined, these changes increase the likelihood of the data for the three-neutrino model and best-fit $3 + 1$ model by, respectively, 0.09 and 0.18 log-likelihood (LLH) units.

Both a frequentist parameter estimation and a pointwise Bayesian model comparison [86] are performed, following the same procedure as in Ref. [48]. The likelihood function and Bayes factor [87] are evaluated over a grid scan of the three physics parameters— Δm_{41}^2 , $\sin^2 2\theta_{24}$, and g^2 —where Δm_{41}^2 and $\sin^2 2\theta_{24}$ are sampled log uniformly with ten samples per decade in the ranges 0.01–47 eV² and 0.01–1.0, respectively, and the parameter g^2 is sampled in steps of $(\pi/2)$ in the range $0 - 4\pi$.

The best-fit parameters are found to be $\Delta m_{41}^2 = 6.7_{-2.5}^{+3.9}$ eV², $\sin^2 2\theta_{24} = 0.33_{-0.17}^{+0.20}$, and $g^2 = 2.5\pi \pm 1.5\pi$. The $\bar{\nu}_\mu$ disappearance probabilities are given in Fig. 1 for the parameters $\Delta m_{41}^2 = 6.7$ eV² and $\sin^2 2\theta_{24} = 0.33$, and for two values of g^2 ; the top panel shows the situation for $g^2 = 0$, which corresponds to the $3 + 1$ model, while the bottom panel is for the case $g^2 = 2.5\pi$. The bottom panel

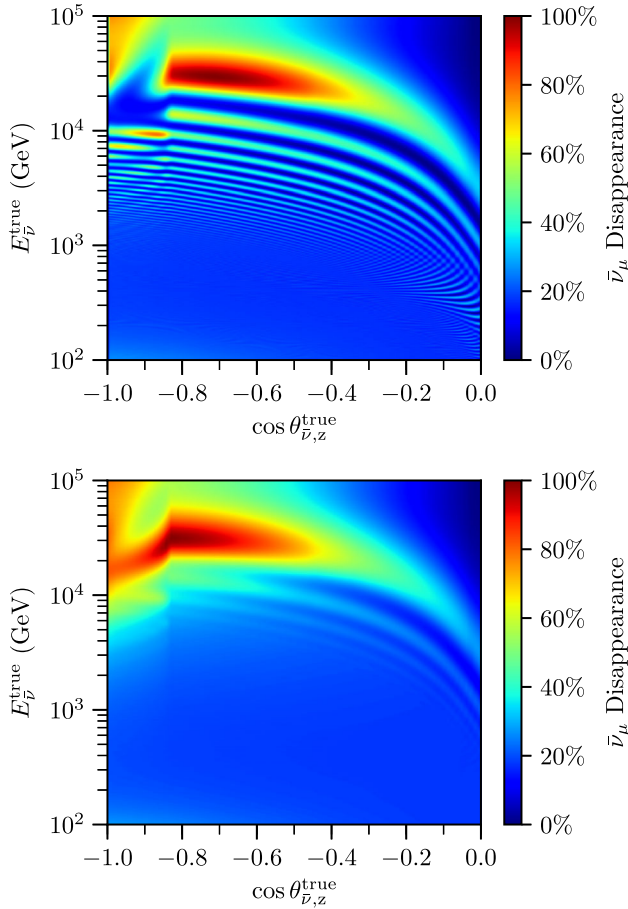


FIG. 1. Muon antineutrino disappearance probabilities for the sterile parameters $\Delta m_{41}^2 = 6.7 \text{ eV}^2$, $\sin^2 2\theta_{24} = 0.33$, and two values of g^2 . Top: $g^2 = 0$, which corresponds to infinite ν_4 lifetime, i.e., the $3 + 1$ model. Bottom: $g^2 = 2.5\pi$; this is the best-fit point.

represents the best-fit point of the frequentist analysis. Muon neutrino disappearance probabilities do not feature the resonant deficit and make subleading contributions to the sterile signature, so they are not shown.

The best-fit signal expectation and data are both compared to the three-neutrino model expectation in Fig. 2. In these plots, both the signal expectation and the three-neutrino model expectation include systematic uncertainties estimated adopting the respective physics parameters. Both the data and the best-fit signal shapes have a deficit of events for through-going neutrinos at the highest energies and a relative excess for horizon-skimming events at the highest energies. The fit values of all systematic uncertainties are within 1σ of their prior centers, with the exception of the cosmic-ray spectral index. The fit value of this systematic uncertainty deviates by 2.4σ , which is similar to both the result from the $3 + 1$ search [47,48], as well as the fit value assuming no sterile neutrino.

The frequentist confidence regions sliced at the best-fit value of g^2 are shown in Fig. 3. The contours are drawn

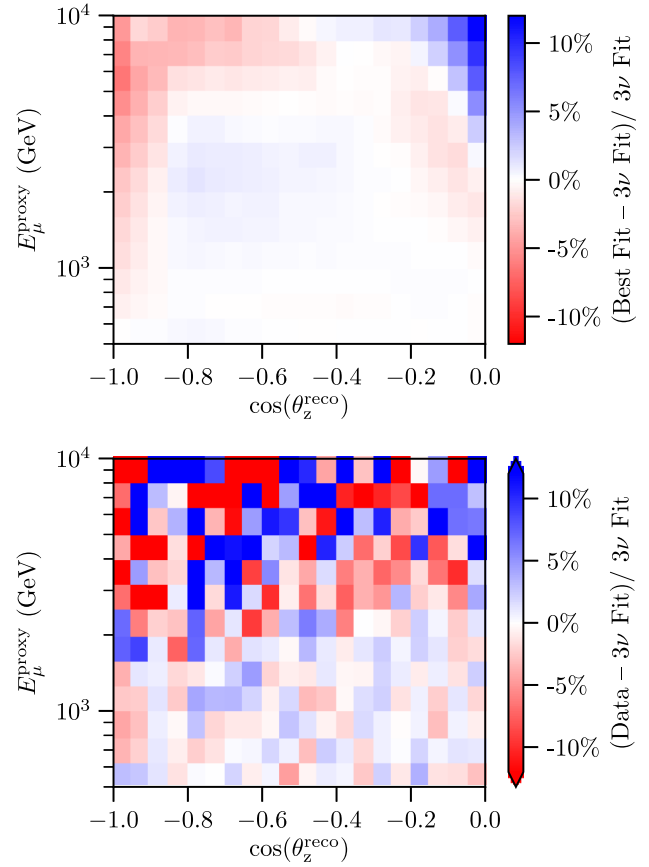


FIG. 2. Top: Comparison of best-fit signal expectation to the three-neutrino fit. Bottom: Comparison of the binned data to the three-neutrino fit. Distributions are binned in reconstructed muon energy (E_μ^{Proxy}) and cosine zenith angle.

assuming Wilks' theorem and three degrees of freedom (DOF). Fits to simulated datasets for several points in the parameter space showed the effective DOF was consistent with three or fewer. The slices of the confidence regions for the other values of g^2 are approximately the same in the 2D space of $[\Delta m_{41}^2, \sin^2 2\theta_{24}]$, with two deviations: the 90% C.L. (confidence level) region for $g^2 = 0$ excludes any point with $\sin^2 2\theta_{24} \gtrsim 0.2$, and above $\Delta m_{41}^2 \sim 7 \text{ eV}^2$, the confidence regions extend to higher Δm_{41}^2 values for larger values of g^2 . This is shown in the Supplemental Material [88]. The effective DOF at the null hypothesis (only three neutrinos) was determined to be 2.86 ± 0.14 , obtained by fitting 300 simulated datasets generated assuming this hypothesis. The null hypothesis is disfavored in favor of the $3 + 1 + \text{decay}$ model with $-2\Delta\text{LLH} = 9.1$ and a p value of 2.8%. This p value was obtained using Wilks' theorem and three DOF, which is conservative and consistent with the DOF assumed for the contours.

The Bayesian analysis finds the best model to have the parameters $\Delta m_{41}^2 = 6.7 \text{ eV}^2$, $\sin^2 \theta_{24} = 0.33$, and $g^2 = 1.5\pi$; this model has a Bayes factor (BF) with respect to the three-neutrino model of 0.025. The Bayes factor of

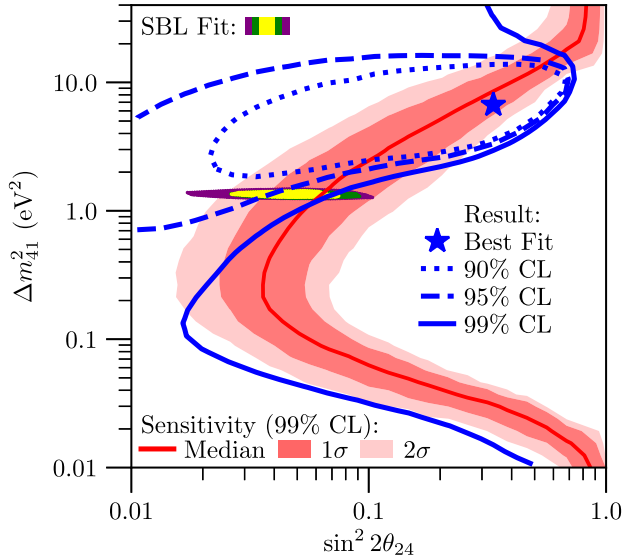


FIG. 3. The result of the frequentist analysis for $g^2 = 2.5\pi$. The 90%, 95%, and 99% C.L. contours are shown as blue dotted, dashed, and solid curves, respectively. The best-fit point is marked with a blue star. The median sensitivity at 99% C.L., determined from 300 simulated datasets, is shown as a red curve. The medium and light pink bands indicate the 1σ and 2σ regions for the sensitivity. The 2D projection of the SBL fit results from [4] for the range $2.25\pi \leq g^2 \leq 2.75\pi$ at 90% C.L., 95% C.L., and 99% C.L. are shown as the solid yellow, green, and purple islands around $\Delta m_{41}^2 = 1.3 \text{ eV}^2$.

the frequentist best-fit point is 0.027. The Bayesian result for $g^2 = 2.5\pi$ is shown in Fig. 4. As with the frequentist confidence regions, Bayesian preferred regions sliced at the varying values of g^2 are very similar, with a few exceptions. For $g^2 = 0$, the region $\log_{10}(\text{BF}) \leq -0.5$ excludes points with $\sin^2 2\theta_{24} \gtrsim 0.2$. The regions with $\log_{10}(\text{BF}) = -1.5$ only occur for $1.5\pi \leq g^2 \leq 2.5\pi$. This is shown in the Supplemental Material [88].

The frequentist and Bayesian results profiled over the parameters Δm_{41}^2 and $\sin^2 2\theta_{24}$ are shown in Fig. 5. Both analyses find some preference for nonzero g^2 . In the frequentist analysis, $g^2 = 0$ is disfavored in favor of nonzero g^2 with $-2\Delta\text{LLH} = 3.9$ and a p value of 0.81%. This p value was obtained using Wilks' theorem and 0.26 effective DOF. The effective DOF was determined by fitting 500 simulated datasets generated assuming the best-fit 3 + 1 parameters, i.e., fixing $g^2 = 0$. The uncertainty of the value of the effective DOF is 0.02.

The 95% C.L. allowed region found in this Letter overlaps that of the SBL fits, as seen in Fig. 3. This overlap occurs to some extent for all nonzero values of g^2 , but is larger for g^2 values above π . This overlap remains fixed in Δm_{41}^2 and $\sin^2 2\theta_{24}$ for varying g^2 . At and above $g^2 = \pi$, there is some overlap between the 95% C.L. region of this Letter and the 90% C.L. allowed region from the SBL fits.

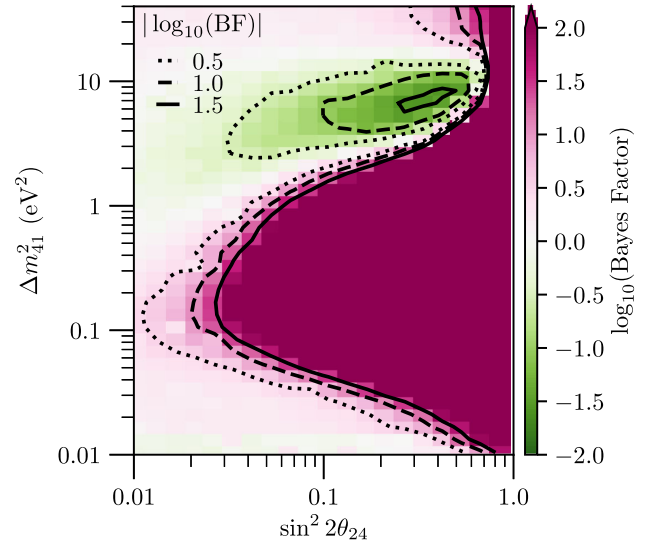


FIG. 4. The result of the Bayesian analysis for $g^2 = 2.5\pi$. The color indicates the logarithm of the Bayes factor with respect to the three-neutrino model; magenta regions have strong preference for the three-neutrino model, while green regions have preference for the sterile neutrino model. The dotted, dashed, and solid black contours correspond to $\log_{10}(\text{BF})$ equaling ± 0.5 , ± 1.0 , and ± 1.5 , respectively.

In conclusion, we have found no substantive evidence for the 3 + 1 + decay model. The null hypothesis of only three neutrinos is disfavored with a p value of 2.8%, and the 3 + 1 model disfavored with a p value of 0.81%. The

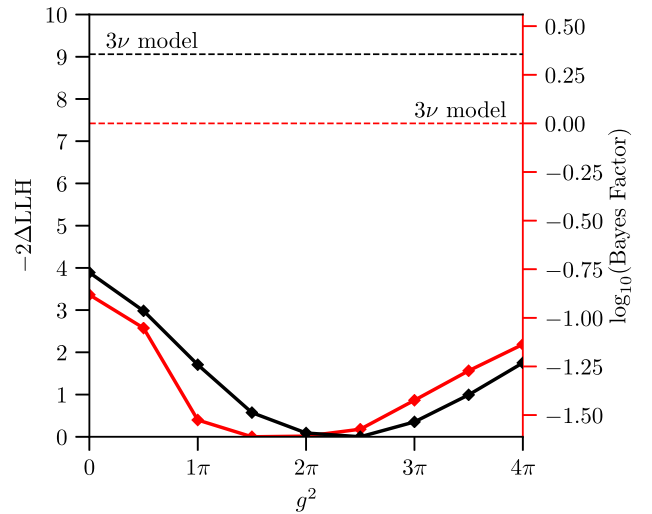


FIG. 5. The frequentist and Bayesian results profiled over two of the sterile parameters, Δm_{41}^2 and $\sin^2 2\theta_{24}$. The frequentist test statistic, $-2\Delta\text{LLH}$ is shown in black and is plotted on the left y axis. The logarithm of the Bayes factor is shown in red and is plotted on the right y axis. The diamond markers joined by the thick lines show the results for the sterile model as a function of the third sterile parameter, g^2 . The results for the null hypothesis—that there are only three neutrino species—are shown in the dashed horizontal lines at the top of the plot.

best-fit parameters are $\Delta m_{41}^2 = 6.7^{+3.9}_{-2.5} \text{ eV}^2$, $\sin^2 2\theta_{24} = 0.33^{+0.20}_{-0.17}$, and $g^2 = 2.5\pi \pm 1.5\pi$. While we have reported valuable new input to global studies, further work, both within and beyond IceCube, is needed to clarify the picture [89]. In particular, in IceCube, the track energy reconstruction can be improved by using machine learning algorithms [90] and the dataset can be expanded to use a new event morphology [91,92].

The IceCube Collaboration acknowledges the significant contributions to this manuscript from the Massachusetts Institute of Technology, University of Texas at Arlington, and Harvard University groups. The authors gratefully acknowledge the support from the following agencies and institutions: USA—U.S. National Science Foundation—Office of Polar Programs, U.S. National Science Foundation—Physics Division, U.S. National Science Foundation—EPSCoR, Wisconsin Alumni Research Foundation, Center for High Throughput Computing (CHTC) at the University of Wisconsin—Madison, Open Science Grid (OSG), Extreme Science and Engineering Discovery Environment (XSEDE), Frontera computing project at the Texas Advanced Computing Center, U.S. Department of Energy—National Energy Research Scientific Computing Center, Particle astrophysics research computing center at the University of Maryland, Institute for Cyber-Enabled Research at Michigan State University, and Astroparticle physics computational facility at Marquette University; Belgium—Funds for Scientific Research (FRS-FNRS and FWO), FWO Odysseus and Big Science programmes, and Belgian Federal Science Policy Office (Belspo); Germany—Bundesministerium für Bildung und Forschung (BMBF), Deutsche Forschungsgemeinschaft (DFG), Helmholtz Alliance for Astroparticle Physics (HAP), Initiative and Networking Fund of the Helmholtz Association, Deutsches Elektronen Synchrotron (DESY), and High Performance Computing cluster of the RWTH Aachen; Sweden—Swedish Research Council, Swedish Polar Research Secretariat, Swedish National Infrastructure for Computing (SNIC), and Knut and Alice Wallenberg Foundation; Australia—Australian Research Council; Canada—Natural Sciences and Engineering Research Council of Canada, Calcul Québec, Compute Ontario, Canada Foundation for Innovation, WestGrid, and Compute Canada; Denmark—Villum Fonden and Carlsberg Foundation; New Zealand—Marsden Fund; Japan—Japan Society for Promotion of Science (JSPS) and Institute for Global Prominent Research (IGPR) of Chiba University; Korea—National Research Foundation of Korea (NRF); Switzerland—Swiss National Science Foundation (SNSF); United Kingdom—Department of Physics, University of Oxford.

*analysis@icecube.wisc.edu

†Also at Università di Padova, I-35131 Padova, Italy.

‡Also at Earthquake Research Institute, University of Tokyo, Bunkyo, Tokyo 113-0032, Japan.

- [1] C. Athanassopoulos, L. B. Auerbach, R. L. Burman, D. O. Caldwell, E. D. Church *et al.* (LSND Collaboration), Evidence for $\nu_\mu \rightarrow \nu_e$ Neutrino Oscillations from LSND, *Phys. Rev. Lett.* **81**, 1774 (1998).
- [2] A. A. Aguilar-Arevalo, B. C. Brown, J. M. Conrad, R. Dharmapalan, A. Diaz *et al.* (MiniBooNE Collaboration), Updated MiniBooNE neutrino oscillation results with increased data and new background studies, *Phys. Rev. D* **103**, 052002 (2021).
- [3] M. Dentler, A. Hernández-Cabezudo, J. Kopp, P. A. N. Machado, M. Maltoni, I. Martinez-Soler, and T. Schwetz, Updated global analysis of neutrino oscillations in the presence of eV-scale sterile neutrinos, *J. High Energy Phys.* **08** (2018) 010.
- [4] A. Diaz, C. A. Argüelles, G. H. Collin, J. M. Conrad, and M. H. Shaevitz, Where are we with light sterile neutrinos?, *Phys. Rep.* **884**, 1 (2020).
- [5] S. Gariazzo, C. Giunti, M. Laveder, and Y. F. Li, Updated global 3 + 1 analysis of short-baseLine neutrino oscillations, *J. High Energy Phys.* **06** (2017) 135.
- [6] M. Maltoni and T. Schwetz, Testing the statistical compatibility of independent data sets, *Phys. Rev. D* **68**, 033020 (2003).
- [7] N. Aghanim *et al.* (Planck Collaboration), Planck 2018 results. VI. Cosmological parameters, *Astron. Astrophys.* **641**, A6 (2020); **652**, C4(E) (2021).
- [8] A. D. Dolgov, Neutrinos in cosmology, *Phys. Rep.* **370**, 333 (2002).
- [9] X. Chu, B. Dasgupta, M. Dentler, J. Kopp, and N. Saviano, Sterile neutrinos with secret interactions—cosmological discord?, *J. Cosmol. Astropart. Phys.* **11** (2018) 049.
- [10] K. N. Abazajian, Sterile neutrinos in cosmology, *Phys. Rep.* **711–712**, 1 (2017).
- [11] S. Hagstotz, P. F. de Salas, S. Gariazzo, S. Pastor, M. Gerbino, M. Lattanzi, S. Vagnozzi, and K. Freese, Bounds on light sterile neutrino mass and mixing from cosmology and laboratory searches, *Phys. Rev. D* **104**, 123524 (2021).
- [12] L. Verde, T. Treu, and A. G. Riess, Tensions between the early and the late universe, *Nat. Astron.* **3**, 891 (2019).
- [13] A. G. Riess, The expansion of the universe is faster than expected, *Nat. Rev. Phys.* **2**, 10 (2020).
- [14] C. D. Kreisch, F.-Y. Cyr-Racine, and O. Doré, Neutrino puzzle: Anomalies, interactions, and cosmological tensions, *Phys. Rev. D* **101**, 123505 (2020).
- [15] E. Di Valentino, A combined analysis of the H_0 late time direct measurements and the impact on the Dark Energy sector, *Mon. Not. R. Astron. Soc.* **502**, 2065 (2021).
- [16] M. Archidiacono, S. Gariazzo, C. Giunti, S. Hannestad, R. Hansen, M. Laveder, and T. Tram, Pseudoscalar—sterile neutrino interactions: Reconciling the cosmos with neutrino oscillations, *J. Cosmol. Astropart. Phys.* **08** (2016) 067.
- [17] M. Ericson, M. V. Garzelli, C. Giunti, and M. Martini, Assessing the role of nuclear effects in the interpretation of

- the MiniBooNE low-energy anomaly, *Phys. Rev. D* **93**, 073008 (2016).
- [18] V. Brdar and J. Kopp, Can standard model and experimental uncertainties resolve the MiniBooNE anomaly?, *Phys. Rev. D* **105**, 115024 (2022).
- [19] C. Giunti, A. Ioannisian, and G. Ranucci, A new analysis of the MiniBooNE low-energy excess, *J. High Energy Phys.* **11** (2020) 146; **02** (2021) 78(E).
- [20] L. Alvarez-Ruso, J. Nieves, and E. Wang, Single photon production induced by (anti)neutrino neutral current scattering on nucleons and nuclear targets, *AIP Conf. Proc.* **1680**, 020002 (2015).
- [21] W. Abdallah, R. Gandhi, and S. Roy, Two-Higgs doublet solution to the LSND, MiniBooNE and muon $g-2$ anomalies, *Phys. Rev. D* **104**, 055028 (2021).
- [22] A. Abdollahi, M. Hostert, and S. Pascoli, A dark seesaw solution to low energy anomalies: MiniBooNE, the muon ($g-2$), and BABAR, *Phys. Lett. B* **820**, 136531 (2021).
- [23] G. Magill, R. Plestid, M. Pospelov, and Y.-D. Tsai, Dipole portal to heavy neutral leptons, *Phys. Rev. D* **98**, 115015 (2018).
- [24] B. J. P. Jones and J. Spitz, Neutrino flavor transformations from new short-range forces, [arXiv:1911.06342](https://arxiv.org/abs/1911.06342).
- [25] E. Bertuzzo, S. Jana, P. A. N. Machado, and R. Zukanovich Funchal, Dark Neutrino Portal to Explain MiniBooNE Excess, *Phys. Rev. Lett.* **121**, 241801 (2018).
- [26] O. Fischer, A. Hernández-Cabezudo, and T. Schwetz, Explaining the MiniBooNE excess by a decaying sterile neutrino with mass in the 250 MeV range, *Phys. Rev. D* **101**, 075045 (2020).
- [27] M. Dentler, I. Esteban, J. Kopp, and P. Machado, Decaying sterile neutrinos and the short baseline oscillation anomalies, *Phys. Rev. D* **101**, 115013 (2020).
- [28] A. de Gouvêa, O. L. G. Peres, S. Prakash, and G. V. Stenico, On the decaying-sterile neutrino solution to the electron (anti)neutrino appearance anomalies, *J. High Energy Phys.* **07** (2020) 141.
- [29] S. N. Gninenko, The MiniBooNE Anomaly and Heavy Neutrino Decay, *Phys. Rev. Lett.* **103**, 241802 (2009).
- [30] M. Carena, Y.-Y. Li, C. S. Machado, P. A. N. Machado, and C. E. M. Wagner, Neutrinos in large extra dimensions and short-baseline ν_e appearance, *Phys. Rev. D* **96**, 095014 (2017).
- [31] M. Masip, P. Masjuan, and D. Meloni, Heavy neutrino decays at MiniBooNE, *J. High Energy Phys.* **01** (2013) 106.
- [32] C. Dib, J. C. Helo, S. Kovalenko, and I. Schmidt, Sterile neutrino decay explanation of LSND and MiniBooNE anomalies, *Phys. Rev. D* **84**, 071301(R) (2011).
- [33] Y. Bai, R. Lu, S. Lu, J. Salvado, and B. A. Stefanek, Three twin neutrinos: Evidence from LSND and MiniBooNE, *Phys. Rev. D* **93**, 073004 (2016).
- [34] Z. Moss, M. H. Moulai, C. A. Argüelles, and J. M. Conrad, Exploring a nonminimal sterile neutrino model involving decay at IceCube, *Phys. Rev. D* **97**, 055017 (2018).
- [35] S. Vergani, N. W. Kamp, A. Diaz, C. A. Argüelles, J. M. Conrad, M. H. Shaevitz, and M. A. Uchida, Explaining the MiniBooNE excess through a mixed model of neutrino oscillation and decay, *Phys. Rev. D* **104**, 095005 (2021).
- [36] M. H. Moulai, C. A. Argüelles, G. H. Collin, J. M. Conrad, A. Diaz, and M. H. Shaevitz, Combining sterile neutrino fits to short baseline data with IceCube data, *Phys. Rev. D* **101**, 055020 (2020).
- [37] M. G. Aartsen *et al.* (IceCube Collaboration), The IceCube neutrino observatory: Instrumentation and online systems, *J. Instrum.* **12**, P03012 (2017).
- [38] R. Abbasi *et al.* (IceCube Collaboration), The IceCube data acquisition system: Signal capture, digitization, and time-stamping, *Nucl. Instrum. Methods Phys. Res., Sect. A* **601**, 294 (2009).
- [39] M. G. Aartsen *et al.* (IceCube Collaboration), Energy reconstruction methods in the IceCube neutrino telescope, *J. Instrum.* **9**, P03009 (2014).
- [40] R. Abbasi *et al.* (IceCube Collaboration), The design and performance of IceCube deepCore, *Astropart. Phys.* **35**, 615 (2012).
- [41] E. K. Akhmedov, Neutrino oscillations in inhomogeneous matter (In Russian), *Yad. Fiz.* **47**, 475 (1988) [*Sov. J. Nucl. Phys.* **47**, 301 (1988)].
- [42] P. I. Krastev and A. Yu. Smirnov, Parametric effects in neutrino oscillations, *Phys. Lett. B* **226**, 341 (1989).
- [43] M. Chizhov, M. Maris, and S. T. Petcov, On the oscillation length resonance in the transitions of solar and atmospheric neutrinos crossing the earth core, [arXiv:hep-ph/9810501](https://arxiv.org/abs/hep-ph/9810501).
- [44] M. V. Chizhov and S. T. Petcov, New Conditions for a Total Neutrino Conversion in a Medium, *Phys. Rev. Lett.* **83**, 1096 (1999).
- [45] E. K. Akhmedov and A. Yu. Smirnov, Comment on ‘New Conditions for a Total Neutrino Conversion in a Medium’, *Phys. Rev. Lett.* **85**, 3978 (2000).
- [46] H. Nunokawa, O. L. G. Peres, and R. Zukanovich Funchal, Probing the LSND mass scale and four neutrino scenarios with a neutrino telescope, *Phys. Lett. B* **562**, 279 (2003).
- [47] M. G. Aartsen *et al.* (IceCube Collaboration), eV-Scale Sterile Neutrino Search Using Eight Years of Atmospheric Muon Neutrino Data from the IceCube Neutrino Observatory, *Phys. Rev. Lett.* **125**, 141801 (2020).
- [48] M. G. Aartsen *et al.* (IceCube Collaboration), Searching for eV-scale sterile neutrinos with eight years of atmospheric neutrinos at the IceCube Neutrino Telescope, *Phys. Rev. D* **102**, 052009 (2020).
- [49] C. W. Kim and W. P. Lam, Some remarks on neutrino decay via a Nambu-Goldstone boson, *Mod. Phys. Lett. A* **05**, 297 (1990).
- [50] P. Zyla *et al.* (Particle Data Group), Review of particle physics, *Prog. Theor. Exp. Phys.* **2020**, 083C01 (2020).
- [51] A. Esmaili and A. Yu. Smirnov, Restricting the LSND and MiniBooNE sterile neutrinos with the IceCube atmospheric neutrino data, *J. High Energy Phys.* **12** (2013) 014.
- [52] M. Lindner, W. Rodejohann, and X.-J. Xu, Sterile neutrinos in the light of IceCube, *J. High Energy Phys.* **01** (2016) 124.
- [53] T. K. Gaisser, Spectrum of cosmic-ray nucleons, kaon production, and the atmospheric muon charge ratio, *Astropart. Phys.* **35**, 801 (2012).
- [54] S. N. G. Axani, Sterile neutrino searches at the IceCube neutrino observatory, Ph.D. thesis, MIT (2019), [arXiv:2003.02796](https://arxiv.org/abs/2003.02796).
- [55] M. G. Aartsen *et al.* (IceCube Collaboration), Evidence for high-energy extraterrestrial neutrinos at the IceCube detector, *Science* **342**, 1242856 (2013).

- [56] M. G. Aartsen *et al.* (IceCube Collaboration), Observation of High-Energy Astrophysical Neutrinos in Three Years of IceCube Data, *Phys. Rev. Lett.* **113**, 101101 (2014).
- [57] M. Aartsen *et al.* (IceCube Collaboration), Evidence for Astrophysical Muon Neutrinos from the Northern Sky with IceCube, *Phys. Rev. Lett.* **115**, 081102 (2015).
- [58] M. G. Aartsen *et al.* (IceCube Collaboration), Observation and characterization of a cosmic muon neutrino flux from the northern hemisphere using six years of IceCube data, *Astrophys. J.* **833**, 3 (2016).
- [59] M. G. Aartsen *et al.* (IceCube Collaboration), Measurements using the inelasticity distribution of multi-TeV neutrino interactions in IceCube, *Phys. Rev. D* **99**, 032004 (2019).
- [60] R. Abbasi *et al.* (IceCube Collaboration), The IceCube high-energy starting event sample: Description and flux characterization with 7.5 years of data, *Phys. Rev. D* **104**, 022002 (2021).
- [61] M. G. Aartsen *et al.* (IceCube Collaboration), Characteristics of the Diffuse Astrophysical Electron and Tau Neutrino Flux with Six Years of IceCube High Energy Cascade Data, *Phys. Rev. Lett.* **125**, 121104 (2020).
- [62] A. Fedynitch, R. Engel, T. K. Gaisser, F. Riehn, and T. Stanev, Calculation of conventional and prompt lepton fluxes at very high energy, *EPJ Web Conf.* **99**, 08001 (2015).
- [63] M. V. Garzelli, S. Moch, and G. Sigl, Lepton fluxes from atmospheric charm revisited, *J. High Energy Phys.* **10** (2015) 115.
- [64] R. Gauld, J. Rojo, L. Rottoli, S. Sarkar, and J. Talbert, The prompt atmospheric neutrino flux in the light of LHCb, *J. High Energy Phys.* **02** (2016) 130.
- [65] R. Gauld, J. Rojo, L. Rottoli, and J. Talbert, Charm production in the forward region: Constraints on the small- x gluon and backgrounds for neutrino astronomy, *J. High Energy Phys.* **11** (2015) 009.
- [66] A. Bhattacharya, R. Enberg, Y. S. Jeong, C. S. Kim, M. H. Reno, I. Sarcevic, and A. Stasto, Prompt atmospheric neutrino fluxes: Perturbative QCD models and nuclear effects, *J. High Energy Phys.* **11** (2016) 167.
- [67] M. V. Garzelli, S. Moch, O. Zenaiev, A. Cooper-Sarkar, A. Geiser, K. Lipka, R. Placakyte, and G. Sigl (PROSA Collaboration), Prompt neutrino fluxes in the atmosphere with PROSA parton distribution functions, *J. High Energy Phys.* **05** (2017) 004.
- [68] V. P. Goncalves and M. V. T. Machado, Saturation physics in ultra high energy cosmic rays: Heavy quark production, *J. High Energy Phys.* **04** (2007) 028.
- [69] R. Enberg, M. H. Reno, and I. Sarcevic, Prompt neutrino fluxes from atmospheric charm, *Phys. Rev. D* **78**, 043005 (2008).
- [70] R. Abbasi *et al.* (IceCube Collaboration), The energy spectrum of atmospheric neutrinos between 2 and 200 TeV with the AMANDA-II Detector, *Astropart. Phys.* **34**, 48 (2010).
- [71] C. A. Argüelles Delgado, J. Salvado, and C. N. Weaver, A simple quantum integro-differential solver (SQuIDS), *Comput. Phys. Commun.* **196**, 569 (2015).
- [72] C. A. Argüelles, J. Salvado, and C. N. Weaver, nuSQuIDS: A toolbox for neutrino propagation, *Comput. Phys. Commun.* **277**, 108346 (2022).
- [73] M. C. Gonzalez-Garcia, F. Halzen, and M. Maltoni, Physics reach of high-energy and high-statistics IceCube atmospheric neutrino data, *Phys. Rev. D* **71**, 093010 (2005).
- [74] J. A. Formaggio and G. P. Zeller, From eV to EeV: Neutrino cross sections across energy scales, *Rev. Mod. Phys.* **84**, 1307 (2012).
- [75] R. Gandhi, C. Quigg, M. H. Reno, and I. Sarcevic, Neutrino interactions at ultrahigh-energies, *Phys. Rev. D* **58**, 093009 (1998).
- [76] B. Zhou and J. F. Beacom, W-boson and trident production in TeV–PeV neutrino observatories, *Phys. Rev. D* **101**, 036010 (2020).
- [77] B. Zhou and J. F. Beacom, Neutrino-nucleus cross sections for W-boson and trident production, *Phys. Rev. D* **101**, 036011 (2020).
- [78] A. Garcia, R. Gauld, A. Heijboer, and J. Rojo, Complete predictions for high-energy neutrino propagation in matter, *J. Cosmol. Astropart. Phys.* **09** (2020) 025.
- [79] F. Halzen and D. Saltzberg, Tau-Neutrino Appearance with a 1000 Megaparsec Baseline, *Phys. Rev. Lett.* **81**, 4305 (1998).
- [80] S. Iyer Dutta, M. H. Reno, I. Sarcevic, and D. Seckel, Propagation of muons and taus at high-energies, *Phys. Rev. D* **63**, 094020 (2001).
- [81] A. M. Dziewonski and D. L. Anderson, Preliminary reference earth model, *Phys. Earth Planet. Interiors* **25**, 297 (1981).
- [82] A. Cooper-Sarkar, P. Mertsch, and S. Sarkar, The high energy neutrino cross-section in the standard model and its uncertainty, *J. High Energy Phys.* **08** (2011) 042.
- [83] C. A. Argüelles, A. Schneider, and T. Yuan, A binned likelihood for stochastic models, *J. High Energy Phys.* **06** (2019) 030.
- [84] Jet Propulsion Laboratory, AIRS/AMSU/HSB Version 6 Level 3 Product User Guide, Version 1.2 (November 2014).
- [85] U. S. Atmosphere, National oceanic and atmospheric administration, *National Aeronautics and Space Administration* (United States Air Force, Washington, DC, 1976).
- [86] S. Gariazzo and O. Mena, Cosmology-marginalized approaches in Bayesian model comparison: The neutrino mass as a case study, *Phys. Rev. D* **99**, 021301(R) (2019).
- [87] U. von Toussaint, Bayesian inference in physics, *Rev. Mod. Phys.* **83**, 943 (2011).
- [88] See Supplemental Material at <http://link.aps.org/supplemental/10.1103/PhysRevLett.129.151801> for the complete scan results for the frequentist and Bayesian analyses.
- [89] M. A. Acero *et al.*, White paper on light sterile neutrino searches and related phenomenology, [arXiv:2203.07323](https://arxiv.org/abs/2203.07323).
- [90] R. Abbasi *et al.*, A convolutional neural network based cascade reconstruction for the IceCube neutrino observatory, *J. Instrum.* **16**, P07041 (2021).
- [91] A. Esmaili, F. Halzen, and O. L. G. Peres, Exploring $\nu_\tau - \nu_s$ mixing with cascade events in DeepCore, *J. Cosmol. Astropart. Phys.* **07** (2013) 048.
- [92] B. R. Smithers, B. J. P. Jones, C. A. Argüelles, J. M. Conrad, and A. Diaz, Cascade appearance signatures of sterile neutrinos at 1–100 TeV, *Phys. Rev. D* **105**, 052001 (2022).